كلية الهندسة بشبرا
FACULTY OF ENGINEERING AT SHOUBRA
ERJ
PRINT ISSN 3009-6049
ONLINE ISSN 3009-6022

ENGINEERING RESEARCH JOURNAL (ERJ)
Volume (53),Issue (3)
July 2024, pp:31-36
https://erjsh.journals.ekb.eg

Analytical Modeling of Cable-Driven Soft Manipulators with Constant Curvature: A Simulation Approach

Sameh Habib [1], Tamer A Khalil [1], Sara G. Seadby [2,*], and Shady A. Maged [3]

[1] Mechanical Department, Faculty of Engineering at Shoubra, Benha University, Cairo, Egypt.
[2] Mechatronics Engineering Department, The Higher Technological Institute, 10th of Ramadan City, Egypt.
[3] Mechatronics Engineering Department, Faculty of Engineering, Ain Shams University, Cairo, Egypt.
**Corresponding author*

E-mail address: sameh.abadir@feng.bu.edu.eg , tamer.abdelraouf@feng.bu.edu.eg , saraseadby@gmail.com , shady.maged@eng.asu.edu.eg

Abstract: Cable-driven continuum robots are important in many disciplines because they are versatile and adaptive, allowing for accurate manipulation in confined situations. This paper presents a simulation-based kinematic modeling approach for a cable-driven soft continuum manipulator. The proposed approach is validated through simulations and workspace analysis, demonstrating its effectiveness in predicting the end-effector pose with an average error of 21.01 mm across the provided manipulator configurations, while also revealing potential variations in accuracy depending on the specific configuration. The analysis involves two independent mappings: a general mapping for the kinematics of continuum robots and a specific mapping tailored to the manipulator design. Both mappings are developed for single and multi-section configurations. The workspace analysis revealed a maximum reachable distance of 84.71 mm for the end-effector, with a workspace volume of approximately 8613.54 mm^3, assuming an ellipsoid workspace approximation. This work aims to provide a framework for kinematic analysis of similar cable-driven soft manipulators and insights into the applicability of piecewise constant curvature (PCC) modeling techniques, while also highlighting the need for further investigation and improvement to address the identified variations in accuracy and enhancing the modeling approach's consistency and robustness across a wider range of operating conditions.

Keywords: continuum robot, PCC, soft manipulator.

1. Introduction

Soft robotics has emerged as a promising field, offering advantages such as adaptability, compliance, and safe interaction with the environment. Within soft robotics, continuum robots have garnered attention due to their ability to navigate complex environments and perform delicate tasks[1]–[3]. Cable-driven continuum robots, in particular, have been extensively explored for their potential in diverse applications, including medical interventions and manipulation tasks[4].

Cable-driven continuum robots utilize flexible structures actuated by cables to achieve smooth, continuous bending motions, mimicking biological systems such as elephant trunks or tentacles. This actuation type allows for high flexibility and precise control of the robot's posture, making it suitable for tasks in constrained environments [1][3]. The cable-driven approach is particularly noted for its ability to transmit forces smoothly across the robot's length, enhancing both the dexterity and adaptability of the manipulator[2], [3], [5].

Recent years have seen substantial studies into continuum robot design, modeling, and control. Cable-driven continuum robots have gained popularity because of their flexibility and ease of manufacture. Several designs have been proposed, including those using universal joint backbones, modular segments, and configurable grippers. Relevant research includes the use of 3D printing for novel fabrication methods[6], the design of modular continuum robot segments[7], the analysis of basic modules in modular continuum manipulators[8], the development of cable-driven hyper-redundant robots[9], [10], and the investigation of cable-driven parallel mechanisms for soft joints[11].

Kinematic modeling is essential for the control and application of continuum robots. A common technique for streamlining the kinematic modeling of continuum robots is the constant curvature assumption[12]. However, this assumption may not accurately represent the robot's shape under external loads or when the cables are not uniformly actuated. To address this issue, various approaches have been proposed, such as the PCC method and the Cosserat rod approach[5], [13], [14]. Furthermore, this work guides modeling tendon-driven continuum robots and benchmarking modeling performance, contributing to the accurate kinematic modeling of cable-driven soft manipulators[15]. This work presents a framework for kinematic modeling, integrating PCC kinematics with finite element analysis, offering a comprehensive approach to cable-driven soft manipulator modeling[16]. Additionally, this approach presents an analytical approach that supports accurate modeling methodologies for the kinematics and dynamics of multiple-backbone continuum robots, relevant to cable-driven soft manipulators[17]. Kinematic analysis of continuum robots consisting of driven flexible rods provides insights into the design and performance of cable-driven soft

manipulators which are discussed in this study[18]. Insights from the design and control of a tendon-driven continuum robot contribute to the understanding of cable-driven soft manipulators, emphasizing control strategies for precise manipulation[19]. Using effective inverse kinematics, this study focuses on creating dexterity evaluation algorithms for continuum robots, offering important insights into the evaluation of cable-driven soft manipulators' performance[20]. Kinematic considerations for cable-driven soft manipulators and insights into practical applications are provided by another research on the application of continuum-style robots, such as an elephant's trunk manipulator[21]. This work addresses general forward kinematics for tendon-driven continuum robots, providing mathematical foundations for precise motion planning in cable-driven soft manipulators[22].

Our contribution to this paper is the development of a simulation-based kinematic modeling approach for a cable-driven soft continuum manipulator using the piecewise constant curvature (PCC) assumption. This approach allows for accurate representation of the manipulator's deformations and enables precise control of its motions. We specifically focus on the kinematic analysis of the manipulator, and workspace evaluation.

To achieve this, we first establish a general mapping between configuration space and task space for continuum robot kinematics. This mapping provides a comprehensive understanding of the manipulator's configuration and its corresponding task-related parameters. Additionally, we develop a specific mapping between actuator space and configuration space tailored to the cable-driven manipulator design. This mapping facilitates the translation of actuator inputs into desired manipulator configurations, enabling precise control of the manipulator's motions.

This is how the manuscript is structured: The cable-driven soft manipulator's construction is detailed in the design of a cable-driven soft continuum manipulator section, followed by the Kinematic Modeling section. Followed by the results and discussion section, Finally, the summaries of the article's major contributions and the discussion of potential directions for future study are detailed in the conclusion and future work sections.

2. DESIGN OF A CABLE-DRIVEN SOFT CONTINUUM MANIPULATOR

In industrial applications, the use of flexible soft manipulators can provide significant advantages. This study presents a novel cable-driven soft continuum manipulator design, consisting of a linear arrangement of rigid elements resembling a row of teeth, as depicted in Figure 1. The manipulator's actuation is achieved through a cable securely fastened inside and retracted by motors.

Three low-friction, high-strength nylon tendon cables, each with a 0.5 mm diameter and 12 cm length, are strategically routed through small tunnels along the edges of the backbone. These cables control the bending of the manipulator. Each nylon tendon cable connects to the tip of the manipulator backbone and passes through a 3D-printed path guide, ensuring smooth cable movement and minimizing friction.

Figure 1 illustrates the front and side views of the proposed cable-driven soft manipulator design, providing dimensional details.

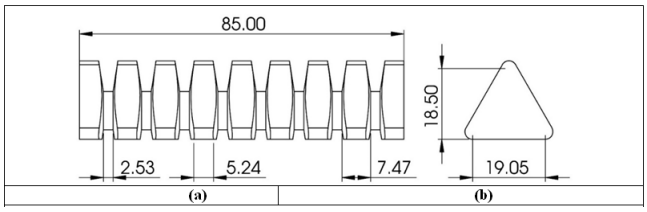

FIGURE 1. Cable-Driven Soft Manipulator Design. (a) Front-View, (b) Side-View(all dimensions in mm).

A comprehensive overview of the manipulator setup, clearly depicting the actuator placement, cable path, and path guide configuration as shown in Fig. 2(a).Furthermore, Fig. 2(b) showcases a fabricated prototype of the proposed manipulator design, either physically printed or simulated in software, allowing for a tangible representation of the concept.

This innovative design leverages the advantages of cable-driven actuation to achieve precise control over the soft continuum manipulator's bending and positioning, making it suitable for various industrial applications that require dexterity and maneuverability in confined spaces.

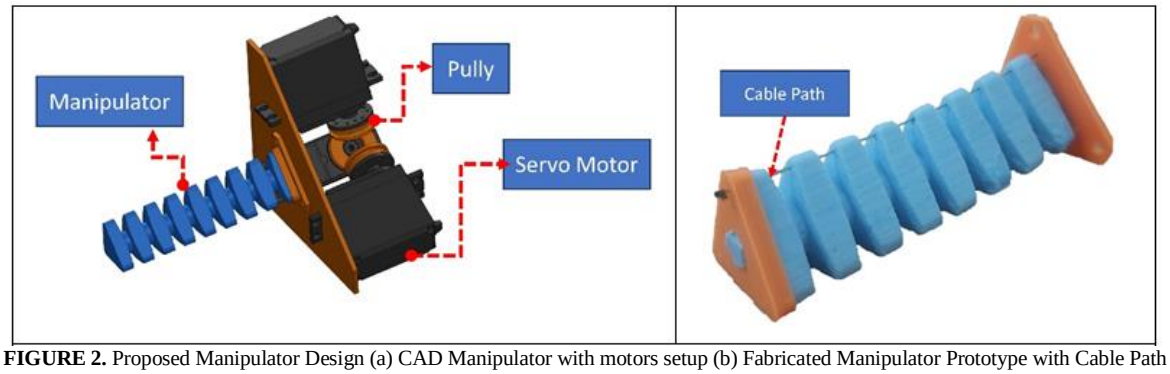

FIGURE 2. Proposed Manipulator Design (a) CAD Manipulator with motors setup (b) Fabricated Manipulator Prototype with Cable Path

3. KINEMATIC MODELING

3.1 Assumptions and Coordinate Frames

The kinematic model is based on the piecewise constant curvature (PCC) approximation where each section of the manipulator bends into a circular arc when actuated. Gravity effects are assumed negligible[23].

As shown in Fig. 3, two mappings are established:

1. Configuration space to task space: Transforming section pose parameters to the end-effector's location and orientation.
2. Actuation space to configuration space: Relating actuator/cable lengths to position and orientation parameters of each section.

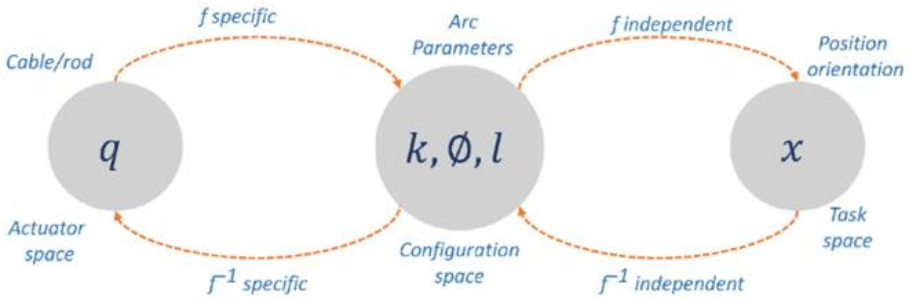

FIGURE 3. The Diagram of the Driven, Joint, and Task Space Mapping.

3.1.1 Broad Mapping of Task Space to Configuration Space

Using constant curvature geometry, homogeneous transformation matrices map the configuration space variables (φ, k, l) to the end-effector pose in task space, where φ represents the rotation angle, k describes the curvature, and l is the arc length. The bending geometry is illustrated in Fig 4. The end effector's location can be learned from Equations (1-3). where θ is the arc angle.

$$x = \cos\varphi\ (1 - \cos kl)/k \quad (1)$$

$$y = \sin\varphi(1 - \cos kl)/k \quad (2)$$

$$z = \sin kl/k \quad (3)$$

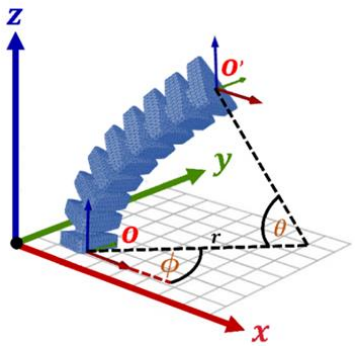

FIGURE 4. Bending Geometry for The Proposed Manipulator.

3.1.2 Particular Mapping of Configuration Space to Actuated Space

For a 3-actuator manipulator, the actuator lengths $q = [l1, l2, l3]$ are related to the arc parameters $l(q), k(q), \varphi(q)$ defining the curved shape, as depicted in Fig. 5. Where the radius of curvature r of the manipulator backbone relates to the radius of curvature ri of each actuator cable, d is the distance from the manipulator center to each actuator center, and φi defines the angular difference between the manipulator's bending plane and actuator $i's$ location.

$$l(q) = (l1 + l2 + l3)/3 \quad (4)$$

$$\varphi(q) = tan^{-1}((\sqrt{3}(l2 + l3 - 2l1))/3(l2 - l3)) \quad (5)$$

$$k(q) = 2\sqrt{l1^2 + l2^2 + l3^2 - l1l2 - l1l3 - l2l3}/d(l1 + l2 + l3) \quad (6)$$

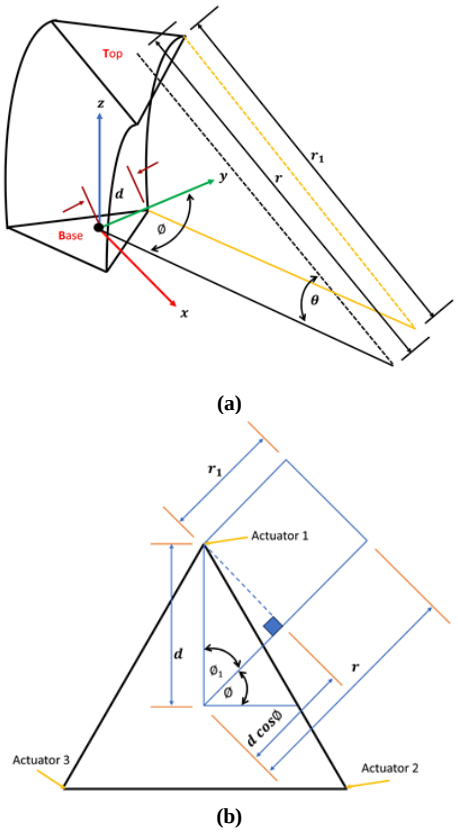

FIGURE 5. (a) The Arc Parameters **(b)** The Base Section Diagram is Viewed from Top.

This maps the actuator space q to the configuration l(q), φ(q), k(q), facilitating forward kinematics from actuator inputs to end-effector pose.

4. RESULTS AND DISCUSSION

In the simulation results, the differential actuation of the three cables caused continuous curvature bending motion, resulting in the manipulator generating an arc shape entirely in the $x-z$ plane. The PCC modeling technique accurately predicted this planar bending profile, with the manipulator backbone adhering to a circular arc specified by the curvature parameter (k) and bending angle (θ). profile, with the manipulator backbone adhering to a circular arc specified by the curvature parameter (k) and bending angle (θ). Fig. 6 depicts the simulated bending behavior of the manipulator when operated with a bending angle of 90 degrees in the $x-z$ plane and a twist angle φ of 0 degrees relative to the x-axis.

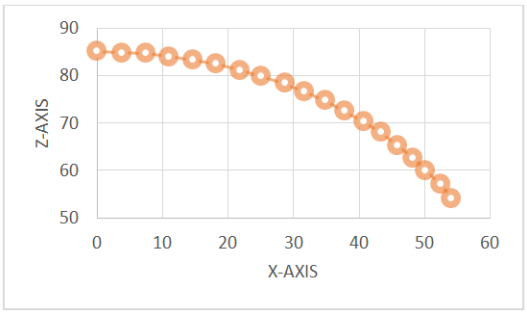

FIGURE 6. Simulation Result

Table 1 and Fig. 7 show the manipulator's shape and end-effector position for different cable lengths (L1,L2,and L3). As the actuator cables are tensioned, the bending angle θ increases, causing the end-effector to trace out a circular trajectory in the x-z plane.

TABLE1: Cable Length Data

Data	Cable lengths (mm)	Tip position (mm)	Position Error(mm)
Data 1	L1=90,l2=70,l3=85	x: -0.00 ,y: -0.00 ,z: 85.00	24.29
Data 2	L1=80,l2=85,l3=90	x: 0.00 ,y: -0.00 ,z: 85.00	12.24
Data 3	L1=75,l2=90,l3=85	x: -0.00 ,y: -0.00 ,z: 83.33	18.27
Data 4	L1=70,l2=95,l3=80	x: -0.00 ,y: -0.00 ,z: 81.67	29.23

The table and output provide the position errors and workspace analysis results for four different configurations of cable lengths. The position error represents the discrepancy between the predicted end-effector position obtained from the kinematic model and the actual end-effector position based on the constant curvature assumption.

For the given configurations, the position errors range from 12.24 mm to 29.23 mm, with an average position error of 21.01 mm across all configurations. The configuration with cable lengths [80, 85, 90] mm exhibits the smallest position error of 12.24 mm, indicating that the kinematic model can accurately predict the end-effector position for this specific configuration. On the other hand, the configuration with cable lengths [70, 95, 80] mm has the largest position error of 29.23 mm, suggesting that the model's accuracy may be lower for certain configurations or operating ranges.

The workspace analysis reveals a maximum reachable distance of 84.71 mm for the end-effector, meaning that the manipulator can reach any point within a spherical workspace with a radius of 84.71 mm from the base. The workspace volume approximated as an ellipsoid, is calculated to be 8613.54 mm^3. This approximation provides an estimate of the total volume of the workspace that the manipulator can access, which can be useful for task planning and design optimization.

It is important to note that the accuracy of the kinematic model and the workspace analysis results may be influenced by various factors, such as modeling assumptions, physical constraints, and the specific manipulator design. Further investigations and refinements may be necessary to improve the model's accuracy and reliability across a wider range of operating conditions.

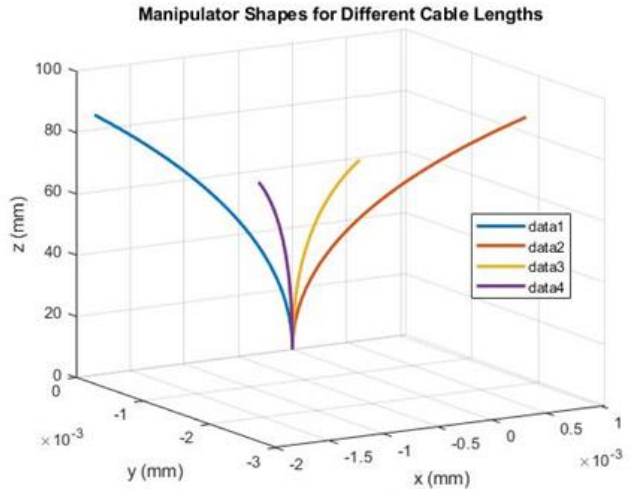

FIGURE 7. Manipulator Shape for Different Cable Lengths

Figure 8 illustrates the manipulator's shape for different bending and twist angles. Fig. 8(a) shows the manipulator without a twist angle, while Fig. 8(b) includes a twist angle.

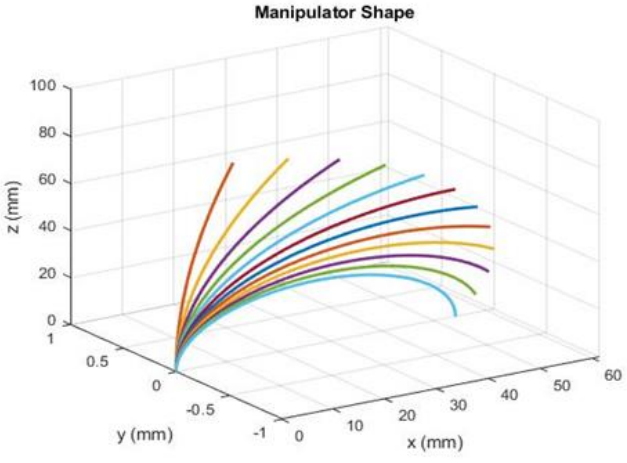

(a)

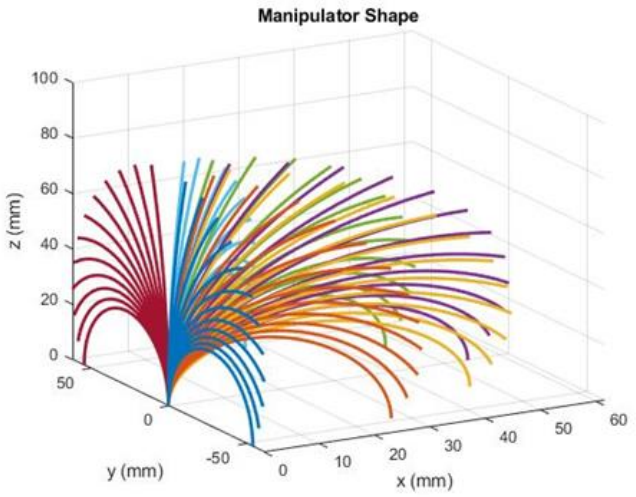

(b)

FIGURE 8. Manipulator Shape for Different Bending and twist angles (a)Without Twist angle, (b) With Twist angle.

The workspace analysis visualized in Fig. 9 reveals the manipulator's reachable end-effector positions, represented by the scatter points within the spherical workspace boundary. The results indicate a roughly spherical workspace. However, because of the physical constraints on the manipulator's bending capabilities at extreme configurations, the possible workspace is not uniformly dense, with smaller coverage at the edges. The operating workspace of the manipulator is better understood thanks to this study, which may also help with job planning and design changes that optimize workspace features for particular uses.

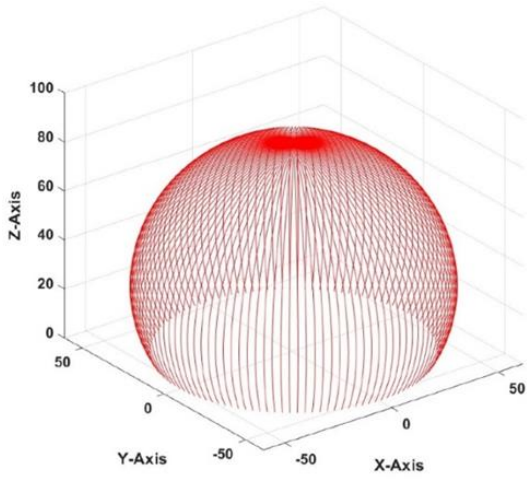

FIGURE 9. Workspace Analysis

5. CONCLUSION AND FUTURE WORK

1. The simulations demonstrated that the proposed kinematic model could predict the end-effector pose with an average position error of 21.01 mm across the provided manipulator configurations.
2. The workspace analysis revealed a maximum reachable distance of 84.71 mm for the end-effector, with a workspace volume of approximately 8613.54 mm^3, assuming an ellipsoid workspace approximation.
3. The kinematic model provides a reasonable approximation of the manipulator's behavior and enables the prediction of the end-effector pose and estimation of the reachable workspace, the results indicate potential variations in accuracy across different configurations.
4. Future work should focus on addressing these variations and improving the model's consistency and robustness across a wider range of operating conditions.

Additionally, employing more sophisticated curved beam finite element representations, data-driven system identification, and adaptive control schemes could further enhance modeling fidelity and account for external loads and non-uniform cable actuation effects. Experimental validation of the physical prototype may also yield valuable insights into the real-world performance of the model and identify prospective avenues for its enhancement.

References

[1] I. D. Walker, “Continuous Backbone ‘Continuum’ Robot Manipulators,” ISRN Robot., vol. 2013, pp. 1–19, 2013, doi: 10.5402/2013/726506.

[2] S. Kolachalama and S. Lakshmanan, “Continuum robots for manipulation applications: A survey,” J. Robot., vol. 2020, 2020, doi: 10.1155/2020/4187048.

[3] M. Russo et al., “Continuum Robots: An Overview,” Adv. Intell. Syst., vol. 5, no. 5, 2023, doi: 10.1002/aisy.202200367.

[4] J. Burgner-Kahrs, D. C. Rucker, and H. Choset, “Continuum Robots for Medical Applications: A Survey,” IEEE Trans. Robot., vol. 31, no. 6, pp. 1261–1280, 2015, doi: 10.1109/TRO.2015.2489500.

[5] P. Schegg and C. Duriez, “Review on generic methods for mechanical modeling, simulation and control of soft robots,” PLoS One, vol. 17, no. 1 January 2022, pp. 1–14, 2022, doi: 10.1371/journal.pone.0251059.

[6] S. K. Mahapatra, A. K. P., and A. Ghosal, “3D printed cable-driven continuum robots with generally routed cables: modeling and experiments,” 2020, [Online]. Available: http://arxiv.org/abs/2003.04593

[7] N. P. Castledine, J. H. Boyle, and J. Kim, “Design of a modular continuum robot segment for use in a general purpose manipulator,” Proc. - IEEE Int. Conf. Robot. Autom., vol. 2019-May, pp. 4430–4435, 2019, doi: 10.1109/ICRA.2019.8794249.

[8] A. K. Mishra, E. Del Dottore, A. Sadeghi, A. Mondini, and B. Mazzolai, “SIMBA: Tendon-driven modular continuum arm with soft reconfigurable gripper,” Front. Robot. AI, vol. 4, no. FEB, pp. 1–10, 2017, doi: 10.3389/frobt.2017.00004.

[9] Z. Li, R. Du, M. C. Lei, and S. M. Yuan, “Design and analysis of a biomimetic wire-driven robot arm,” ASME 2011 Int. Mech. Eng. Congr. Expo. IMECE 2011, vol. 7, no. PARTS A AND B, pp. 191–198, 2011, doi: 10.1115/imece2011-63482.

[10] L. Tang, J. Wang, Y. Zheng, G. Gu, L. Zhu, and X. Zhu, “Design of a cable-driven hyper-redundant robot with experimental validation,” Int. J. Adv. Robot. Syst., vol. 14, no. 5, pp. 1–12, 2017, doi: 10.1177/1729881417734458.

[11] L. Huang, B. Liu, L. Yin, P. Zeng, and Y. Yang, “Design and validation of a novel cable-driven hyper-redundant robot based on decoupled joints,” J. Robot., vol. 2021, 2021, doi: 10.1155/2021/5124816.

[12] M. W. Hannan and I. D. Walker, “Novel Kinematics for Continuum Robots,” Adv. Robot Kinemat., pp. 227–238, 2000, doi: 10.1007/978-94-011-4120-8_24.

[13] [13] C. Della Santina, C. Duriez, and D. Rus, “Model-Based Control of Soft Robots: A Survey of the State of the Art and Open Challenges,” IEEE Control Syst., vol. 43, no. 3, pp. 30–65, 2023, doi: 10.1109/MCS.2023.3253419.

[14] C. Armanini, F. Boyer, A. T. Mathew, C. Duriez, and F. Renda, "Soft Robots Modeling: A Structured Overview," IEEE Trans. Robot., pp. 1–20, 2023, doi: 10.1109/TRO.2022.3231360.

[15] P. Rao, Q. Peyron, S. Lilge, and J. Burgner-Kahrs, "How to Model Tendon-Driven Continuum Robots and Benchmark Modelling Performance," Front. Robot. AI, vol. 7, no. February, pp. 1–20, 2021, doi: 10.3389/frobt.2020.630245.

[16] G. Runge, M. Wiese, L. Gunther, and A. Raatz, "A framework for the kinematic modeling of soft material robots combining finite element analysis and piecewise constant curvature kinematics," 2017 3rd Int. Conf. Control. Autom. Robot. ICCAR 2017, no. April, pp. 7–14, 2017, doi: 10.1109/ICCAR.2017.7942652.

[17] B. He, Z. Wang, Q. Li, H. Xie, and R. Shen, "An analytic method for the kinematics and dynamics of a multiple-backbone continuum robot," Int. J. Adv. Robot. Syst., vol. 10, 2013, doi: 10.5772/54051.

[18] Y. Tian, M. Luan, X. Gao, W. Wang, and L. Li, "Kinematic analysis of continuum robot consisted of driven flexible rods," Math. Probl. Eng., vol. 2016, 2016, doi: 10.1155/2016/6984194.

[19] M. Li, R. Kang, S. Geng, and E. Guglielmino, "Design and control of a tendon-driven continuum robot," vol. 40, no. 11, pp. 3263–3272, 2018, doi: 10.1177/0142331216685607.

[20] F. Du, G. Zhang, Y. Xu, Y. Lei, R. Song, and Y. Li, "Continuum robots: Developing dexterity evaluation algorithms using efficient inverse kinematics," Meas. J. Int. Meas. Confed., vol. 216, no. March, p. 112925, 2023, doi: 10.1016/j.measurement.2023.112925.

[21] M. W. Hannan and I. D. Walker, "Kinematics and the implementation of an elephant's trunk manipulator and other continuum style robots," J. Robot. Syst., vol. 20, no. 2, pp. 45–63, 2003, doi: 10.1002/rob.10070.

[22] M. Moradi Dalvand, S. Nahavandi, and R. D. Howe, "General Forward Kinematics for Tendon-Driven Continuum Robots," IEEE Access, vol. 10, pp. 60330–60340, 2022, doi: 10.1109/ACCESS.2022.3180047.

[23] R. J. Webster and B. A. Jones, "Design and kinematic modeling of constant curvature continuum robots: A review," Int. J. Rob. Res., vol. 29, no. 13, pp. 1661–1683, 2010, doi: 10.1177/0278364910368147.